Piezotronic Effect on the Output Voltage of P3HT/ZnO Micro/Nanowire Heterojunction Solar Cells

ARTICLE *in* NANO LETTERS · SEPTEMBER 2011

Impact Factor: 13.59 · DOI: 10.1021/nl202648p · Source: PubMed

6 AUTHORS, INCLUDING:

Ya Yang
Chinese Academy of Sciences
51 PUBLICATIONS **1,650** CITATIONS
SEE PROFILE

Wenxi Guo
Chinese Academy of Sciences
29 PUBLICATIONS **1,112** CITATIONS
SEE PROFILE

Yan Zhang
Beijing Institute of Technology
872 PUBLICATIONS **11,249** CITATIONS
SEE PROFILE

Yong Ding
Georgia Institute of Technology
128 PUBLICATIONS **13,436** CITATIONS
SEE PROFILE

NANO LETTERS

LETTER

pubs.acs.org/NanoLett

Piezotronic Effect on the Output Voltage of P3HT/ZnO Micro/Nanowire Heterojunction Solar Cells

Ya Yang, Wenxi Guo, Yan Zhang, Yong Ding, Xue Wang, and Zhong Lin Wang*

School of Material Science and Engineering, Georgia Institute of Technology, Atlanta, Georgia 30332-0245, United States

Supporting Information

ABSTRACT:

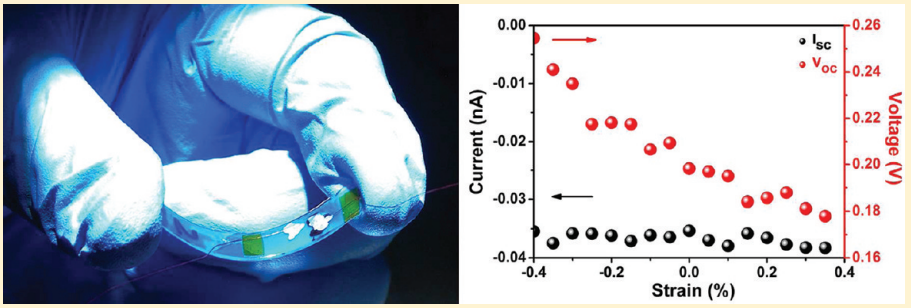

We report the first observation of piezotronic effect on the output voltage of a flexible heterojunction solar cell. The solar cell was fabricated by contacting poly(3-hexylthiophene) (P3HT) with one end of a ZnO micro/nanowire to form a p−n heterojunction on a flexible polystyrene (PS) substrate. The open-circuit voltage V_{oc} of the solar cell was characterized by tuning the strain-induced polarization charges at the interface between ZnO and P3HT. The experimental data were understood based on the modification of the band structure at the p−n junction by the piezopotential, which is referred as a result of the piezotronic effect. This study not only provides an in-depth understanding about the effect but also is useful for maximizing the output of a solar cell using wurtzite structured materials.

KEYWORDS: ZnO micro/nanowires, P3HT, piezopotential, piezotronic effect

One-dimensional semiconducting micro/nanomaterials have potential applications in sensors,[1,2] electronics,[3,4] and photonics.[5,6] Due to the unique semiconducting, piezoelectric, and optoelectronic properties, ZnO micro/nanowires have been extensively used to fabricate field effect transistors,[7,8] ultraviolet lasers,[9] light-emitting diodes,[10] and solar cells.[11] Most interestingly, by utilizing coupled semiconducting and piezoelectric properties of ZnO, some piezoelectric devices including nanogenerators,[12] piezoelectric diodes,[13,14] piezoelectric field effect transistors,[15,16] and piezoelectric strain sensors based on single ZnO micro/nanowires have been successfully demonstrated.[17] Piezotronic effect is to use the inner-crystal piezopotential generated by strain to tune/control the charge transport across a metal−semiconductor junction or a pn junction. The piezotronic devices are based on the modification of piezopotential on the charge transport at metal−semiconductor interface and p−n junction. With the introduction of piezopotential, the performances of some conventional devices can be effectively modulated and optimized.[18−20] Piezotronics is likely to have extensive applications in flexible electronics, biomechanics, and CMOS interfacing and sensors.

The polymer/metal oxide heterojunction solar cell is a promising photovoltaic (PV) technology, offering environmental stability, low cost manufacturing, and versatile applicability.[21] Usually, an inorganic n-type semiconductor (such as TiO_2, ZnO) is interfaced with a p-type organic semiconducting polymer (such as poly(3-hexylthiophene) (P3HT)).[22,23] When light is absorbed by P3HT, the electron−hole pairs are separated at the heterojunction, resulting in the observed photocurrent and photovoltage. Since ZnO is an inexpensive and adaptable material with good stability and high electron mobility, it is particularly attractive to fabricate heterojunction solar cells based on ZnO micro/nanomaterials.[24,25] Although P3HT/ZnO heterojunction based solar cells have been investigated,[26−28] there is a great potential for integrating this type of energy devices on flexible substrates. Inevitably, strain is introduced in the device, which may strongly affect the output of the solar cells.

In this paper, we study the piezotronic effect on the output of a solar cell fabricated by using P3HT and ZnO micro/nanowire, as a model system. The device was packaged by a poly(dimethylsiloxane) (PDMS) thin layer on a PS substrate. The output voltage and current of the solar cell were studied by applying a controlled strain. The results were interpreted based on the principle of piezotronics. These investigations are important for fully understanding the piezotronic effect on energy devices and enhancing the performance of flexible solar cells.

Received: August 1, 2011
Revised: September 17, 2011

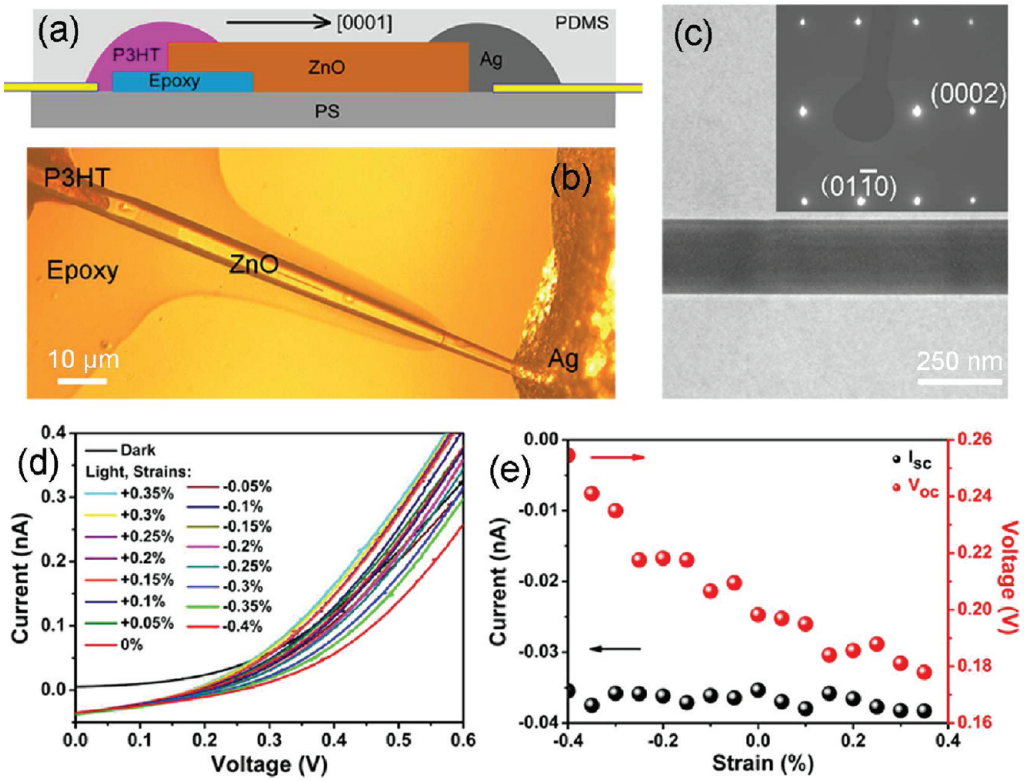

Figure 1. (a) Schematic of a fabricated device of the [0001] type. (b) Optical image of the fabricated device. (c) A TEM image of a single ZnO nanowire and the corresponding selected area electron diffraction (SAED) pattern. (d) $I-V$ characteristics of the device under different strain. (e) Dependence of short-circuit current I_{sc} and the open-circuit voltage V_{oc} on applied strain.

A schematic of the device is shown in Figure 1a. The PS substrate has a length of 4 cm, width of 8 mm, and thickness of 0.5 mm. The ZnO micro/nanowires were synthesized by a high temperature thermal evaporation process, following the procedure described by Pan et al.[29] A scanning electron microscopy (SEM) image of ZnO micro/nanowires shows that the typical length is about several hundred micrometers (Figure S1 in Supporting Information). The long ZnO microwires were chosen because they are easy to manipulate, but the same process applies to nanowires. To avoid the movement of ZnO wire in the electromechanical measurement process, the bottom at one end of the ZnO wire was fixed by a thin epoxy paint film on the PS substrate under optical microscopy. The P3HT in C_6H_5Cl solution was then dropped on the fixed end of the ZnO wire to produce the p−n heterojunction. The ZnO wire was not completely covered by the P3HT (Figure S2 in Supporting Information). The other end of the ZnO wire was fixed by silver paste, serving as an electrode. The device was then packaged by a thin layer of PDMS to prevent the ZnO wire from contamination. Figure 1b shows an optical image of a fabricated device, showing that a smooth ZnO wire was connected by P3HT and silver paste on the substrate. The used ZnO micro/nanowires have a wurtzite structure and grow along the [0001] direction by the transmission electron microscopy (TEM) analysis, as shown in Figure 1c.

The measuring system of the device is shown in Figure S3 in the Supporting Information. One end of the device was fixed tightly on a sample holder with the other end free to be mechanically bent. The tensile and compressive strains were produced by using a three-dimensional mechanical stage (the displacement resolution of 1 μm) to bend the free end of the device. Under AM 1.5 illumination with 100 mW/cm^2 light intensity, the performances of the device with the different strains were measured by a computer-controlled measurement system. To obtain a constant area of light illumination under the different strains, the applied strain was lower than 0.4% to minimize the degree of deformations of the device. The device was illuminated by sunlight through the PS substrate, ZnO wire, P3HT, and PDMS film. Figure 1d shows a photovoltaic performance of the device at different strains under light illumination. The V_{oc} of the device without strains is 0.198 V, which is consistent with literature value of P3HT/ZnO solar cells (0.2 V).[26] The V_{oc} decreases and increases with increasing tensile and compressive strains, respectively.

In a controlled experiment, we measured the $I-V$ characteristics of Ag−ZnO−Ag under dark and light conditions (Figure S4 in Supporting Information). The result shows that there is no observed solar cell performance of this structure, indicating that the photovoltaic performance in Figure 1d is due to the P3HT/ZnO p−n heterojunction rather than the contact between Ag and ZnO.

Since the thickness and the length of the ZnO wire are much smaller than those of PS substrate, the bending of the PS substrate can produce solely a tensile or compressive strain in the ZnO wire depending on its bending directions.[17] The strains induced in the ZnO wire can be obtained by using the deformation of the substrate (calculation of strain in Supporting Information).[17−19,30] The short-circuit current I_{sc} and V_{oc} under the different strains are shown in Figure 1e. The V_{oc} increases and decreases with increasing the compressive and tensile strains, respectively. However, the I_{sc} almost shows a constant value of 0.035 nA under the different strains. The $I-V$ characteristics of another

dx.doi.org/10.1021/nl202648p |*Nano Lett.* XXXX, XXX, 000–000

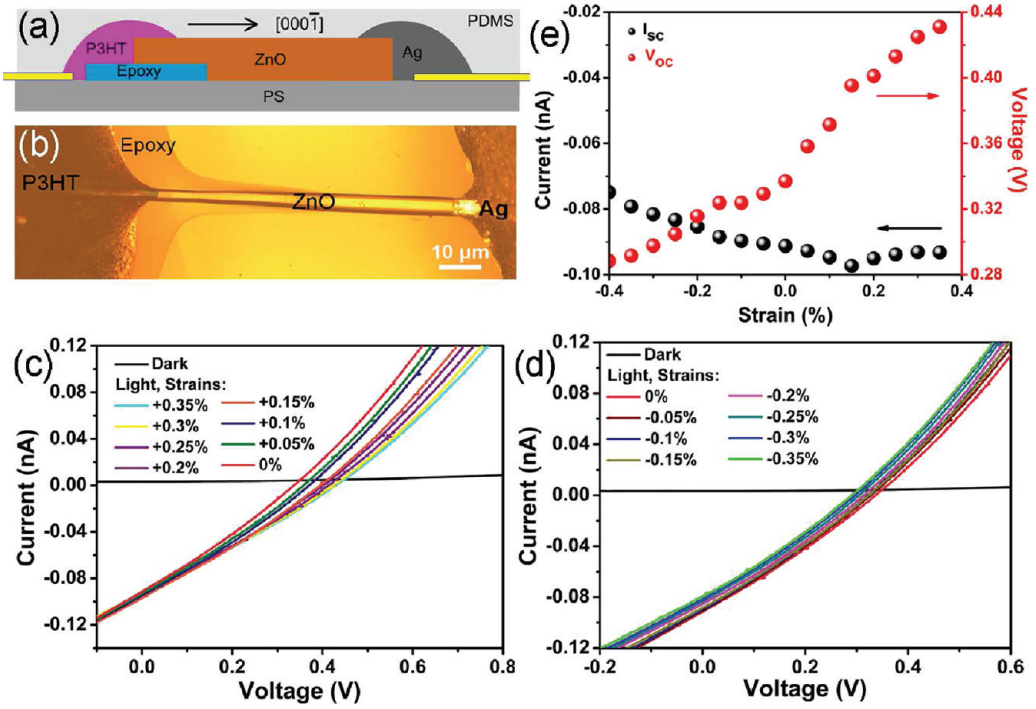

Figure 2. (a) Schematic of a fabricated device of the [000$\bar{1}$] type. (b) Optical image of the fabricated device. (c, d) $I-V$ characteristics of the device under the tensile and compressive strain. (e) Dependence of I_{sc} and V_{oc} on applied strain.

Table 1. The I_{sc}, V_{oc} at Different Strains, and the Corresponding $\Delta V_{oc}/V_{oc}$ of the Fabricated 11 Devices of [0001] and [000$\bar{1}$] Types

type	sample	I_{sc} (nA) [0 strain]	V_{oc} (V) [0 strain]	V_{oc} (V) [compressive (−0.35%) / tensile (0.35%) strain]	$\Delta V_{oc}/V_{oc}$ (max) [compressive (−0.35%) / tensile (0.35%) strain]
[0001]	1	−0.035	0.198	**0.241**/0.178	**22%**/−10%
	2	−0.049	0.282	**0.332**/0.256	**18%**/−9%
	3	−0.050	0.262	**0.362**/0.236	**38%**/-10%
	4	−0.010	0.154	**0.195**/0.142	**21%**/-8%
	5	−0.093	0.363	**0.372**/0.353	**2%**/-3%
[000$\bar{1}$]	6	−0.090	0.337	0.292/**0.431**	−13%/**28%**
	7	−0.200	0.495	0.435/**0.559**	−12%/**25%**
	8	−0.246	0.268	0.257/**0.306**	−4%/**14%**
	9	−0.090	0.331	0.273/**0.383**	−18%/**16%**
	10	−0.151	0.378	0.313/**0.417**	−17%/**10%**
	11	−0.149	0.377	0.325/**0.423**	−14%/**12%**

device with different strains are shown in Figure S5 in the Supporting Information.

Since ZnO has a noncentral symmetric crystal structure with a polar direction along its c axis, there are two ways to contact the P3HT with ZnO wire growing along [0001]. The first way is shown in Figure 1a, where the direction from P3HT to ZnO is along [0001]. The other way is shown in Figure 2a, where the direction from P3HT to ZnO is along [000$\bar{1}$]. Figure 2b shows an optical image of the fabricated device of the [000$\bar{1}$] type. As shown in panels c and d of Figure 2, the $I-V$ characteristics of the devices show an opposite changing trend with the applied strains as compared with those in Figure 1d. Figure 2e shows that the V_{oc} increases and decreases with increasing tensile and compressive strains, respectively. The I_{sc} shows almost a constant value of 0.09 nA under the tensile strain and a slight decrease under the compressive strain. A slight decrease of the I_{sc} may be associated with the increase of ZnO resistance due to compressive strain. The $I-V$ characteristics of another device of this type with different strain are shown in Figure S6 in the Supporting Information, which is consistent with the results presented in Figure 2. We listed the measured results for a total of 11 fabricated devices in Table 1 for presenting the consistency of the measured data. The output power of the solar cells can be maximized by applying a proper strain in the device. When a −0.35% strain is applied on the device, the V_{oc} can be enhanced by 38% as compared with that without strain (Table 1). There are five devices of [0001] case and six devices of [000$\bar{1}$] case. It can be clearly seen that the change tendencies of V_{oc} with the strains are opposite for the two types of contact orientations.

As a p−n heterojunction solar cell, the fabricated device can be described by a Shockley equivalent circuit.[31] The open-circuit

dx.doi.org/10.1021/nl202648p |*Nano Lett.* XXXX, XXX, 000–000

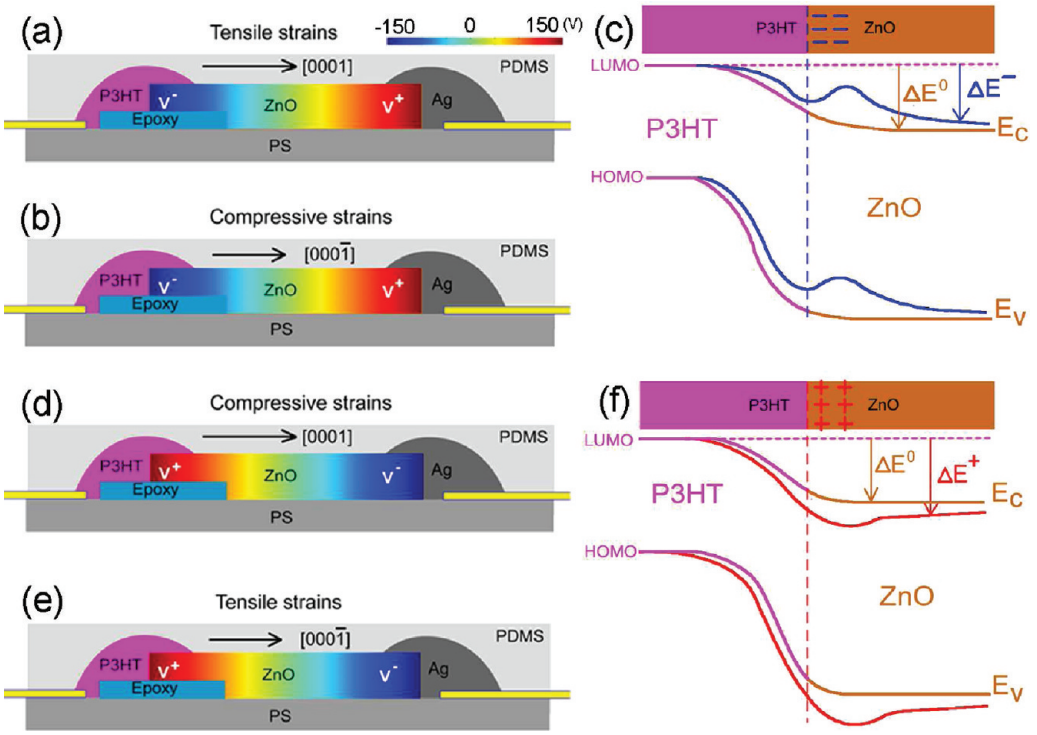

Figure 3. (a, b) The piezopotential distributions in the stretched device of [0001] type and compressed device of [000$\bar{1}$] type. (c) Schematic energy band diagram of P3HT/ZnO with the presence of negative piezoelectric charges. The blue line indicates the modified energy band diagram by the piezoelectric potential in ZnO. The negative piezoelectric charges can lift up the energy band, resulting in a peak in the energy band. (d, e) Calculated piezopotential distributions in the compressed device of [0001] type and stretched device of [000$\bar{1}$] type. (f) Schematic energy band diagram of P3HT/ZnO with the presence of positive piezoelectric charges. The red line represents the modified energy band diagram of ZnO under compressive strain.

voltage V_{oc} and the reverse saturation current I_0 can be then expressed as

$$V_{oc} = n\frac{kT}{e}\ln\left(\frac{I_{sc}}{I_0}\right) \quad (1)$$

$$I_0 = I_{00}\exp\left(\frac{-\Delta E}{rkT}\right) \quad (2)$$

where I_{sc} is the short-circuit current, I_{00} is a prefactor, r is an ideality factor, and ΔE is the energy band difference between the conduction band of a n-type inorganic material and the lowest unoccupied molecular orbit (LUMO) of a p-type organic material.[32,33] By combining eqs 1 and 2, the open-circuit voltage V_{oc} can be given by

$$eV_{oc} = \frac{n}{r}\Delta E + nkT\ln\left(\frac{I_{sc}}{I_{00}}\right) \quad (3)$$

Equation 3 indicates that the open-circuit voltage V_{oc} is associated with both the energy band difference ΔE and the short-circuit current I_{sc}. In our experiment, the I_{sc} is almost constant, and the change of V_{oc} suggests that ΔE may change at the junction area under different strains, in agreement with the result expected from the piezotronic model, to be presented.

Usually, when the ZnO semiconductor material is subjected to strain, the change of the energy band at the interface is associated with the piezoresistance effect and piezoelectric effect.[15,34] For the piezoresistance effect, it has been reported that the tensile strain in a single ZnO wire along the direction of [0001] can decrease the band gap of ZnO,[35] which could increase the ΔE and the V_{oc}. However, since piezoresistance effect is a nonpolar and symmetric effect, it can only result in a similar trend of change of V_{oc} for the fabricated devices of [0001] and [000$\bar{1}$] types, which cannot explain the experimental results presented in Figures 1 and 2. For the piezoelectric effect, it has been extensively reported that the strained ZnO micro/nanowire can change the local energy band profile, resulting in a modulation of $I-V$ characteristics.[17,19,36] According to the fundamental theory of piezotronics,[37] the energy band profile of p−n junction at the interface can be effectively tuned by the strain-induced piezoelectric polarization charges. The piezoelectric polarization charges modify the potential profile at the junction area, resulting in a change of energy band at the p−n junction.[38]

We calculated the distribution of piezopotential in a single ZnO wire with a growth direction of [0001]/[000$\bar{1}$] by using the Lippman theory,[39,40] as shown in Figure 3. For simplicity of the calculation, we ignore the doping in ZnO so that it is assumed to be an insulator. The diameter and length of the ZnO wire are 1 and 10 μm, respectively. The tensile and compressive strains are 0.1% and −0.1%, respectively. Although the calculated piezopotential at the end of ZnO wire is up to 150 V, the actual piezopotential in ZnO is much lower due to the screening effect of the free charge carriers.[39,41] When the ZnO wire was stretched along the c-axial direction, it can create a polarization of cations and anions along the c-axial direction and result in a piezopotential change from V_- to V_+ along the ZnO wire, as shown in Figure 3a. On the basis of the above discussions and calculation of piezopotential, the modulation effect of the strain on the V_{oc} of the fabricated device, as shown in Figures 1 and 2, can then be

dx.doi.org/10.1021/nl202648p |Nano Lett. XXXX, XXX, 000–000

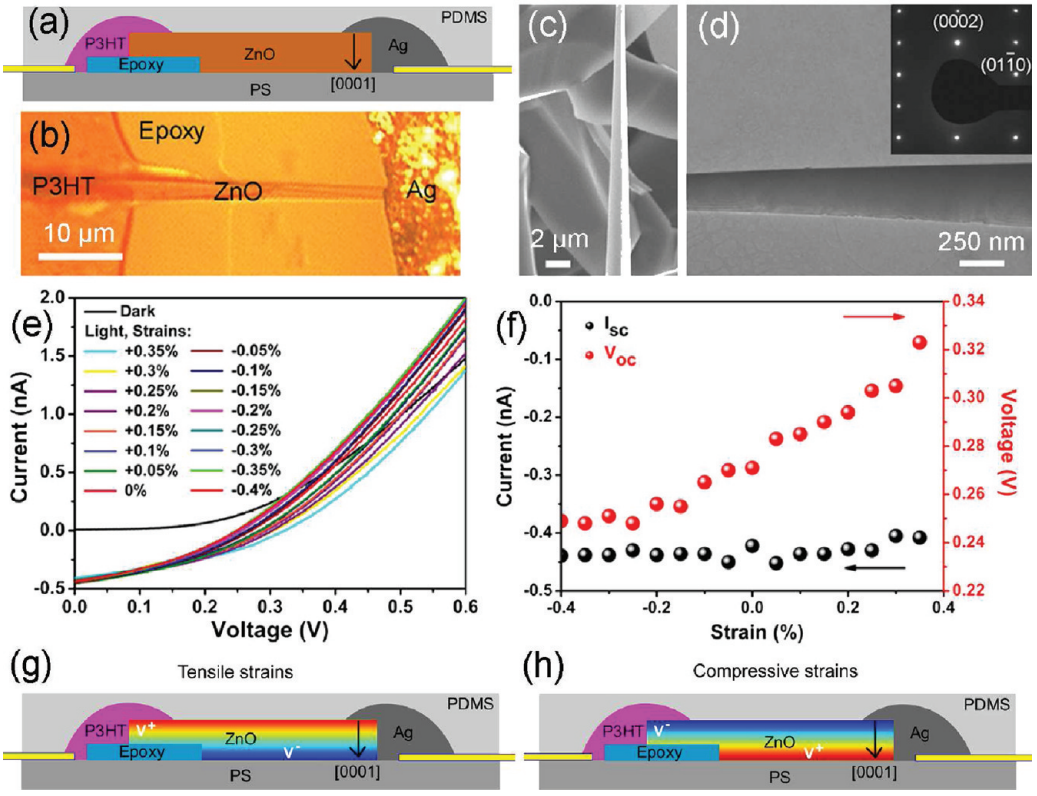

Figure 4. (a) Schematic of a fabricated device based on a single triangular ZnO wire that grows along [01$\bar{1}$0]. (b) Optical image of the fabricated device. (c) SEM image of a single triangular ZnO wire. (d) A TEM image of a single triangular ZnO nanowire and the corresponding SAED pattern. (e) $I-V$ characteristics of the device under different strain. (f) Dependence of I_{sc} and V_{oc} on applied strain. (g) Piezopotential distribution in the tensile strained device. (h) Piezopotential distribution in the compressive strained device.

understood and explained by using the band diagram of the P3HT/ZnO heterojunction at the interface (Figure 3, panels c and f). Considering the result shown in Figure S2 (Supporting Information) that the P3HT is in contact only with the top side of the wire, we can build the following model for understanding our measured results. When a device of [0001] type is under the tensile strain (Figure 3a) or a device of [000$\bar{1}$] type is under compressive strains (Figure 3b), the negative piezopotential is in contact with the P3HT. The negative piezoelectric polarization charges at the interface lift the local conduction band level of ZnO, which can result in a decrease of ΔE and V_{oc} according to eq 3 (ΔE^- as shown in Figure 3c). Moreover, for the cases in Figures 3d and 3e, the positive piezoelectric polarization charges at the interface can lower the local conduction band level of ZnO, resulting in an increase of ΔE and V_{oc} (ΔE^+ as shown in Figure 3f).

Since the growth direction of the ZnO NWs can also be along other crystallographic directions, we investigated the devices fabricated using this type of NW. Figure 4a shows the schematic of another device, where a single triangle ZnO wire was used. The optical image of the device is shown in Figure 4b. The triangle cross section of the ZnO wire can be clearly seen from the SEM and atomic force microscopy (AFM) images (Figure 4c, Figures S7 and S8 in Supporting Information). The TEM image indicates that the triangle ZnO wire has a growth direction along the [01$\bar{1}$0] and a width direction of [0001]. When such a wire is under a tensile/compressive strain along its axial direction, a compressive/tensile strain is created across the width of the ZnO wire; i.e., a strain is induced along the c axis [0001] of the wire, resulting in a piezopotential drop across the width of the ZnO wire.

Figure 4e shows the $I-V$ characteristics of the device at different strains. The corresponding relationships between I_{sc}/V_{oc} and strains are shown in Figure 4f, indicating that the V_{oc} increases and decreases with increasing tensile and compressive strains, respectively. The I_{sc} shows almost a constant value of 0.43 nA. According to the theory of piezotronics, the tensile strains can induce positive and negative piezopotentials at the top and bottom of the ZnO wire, respectively. As shown in Figure 4g, the positive piezopotential is in contact with the P3HT under the tensile strains, resulting in an increase of ΔE and V_{oc}. Moreover, the negative piezopotential can result in a decrease of ΔE and V_{oc}, as shown in Figure 4h. The results are consistent with those in Figures 1 and 2, confirming that the modulation of V_{oc} by the strains is due to piezoelectric effect.

In summary, using P3HT/ZnO micro/nanowire p−n heterojunction on a PS substrate as a model system, we have demonstrated the piezotronic effect on the output voltage of the flexible solar cells for the first time. The strain-induced piezopotential is created under an externally applied strain as a result of piezotronic effect, which tunes the energy band profile at the interface of the p−n heterojunction, consequently modulating the performance of the device. The output power of solar cells could be enhanced by tuning the strains in the devices. Our study not only adds further understanding about piezotronic devices but also shows that it can be applied to enhance their performance of solar cells fabricated by using wurtzite structured materials.

dx.doi.org/10.1021/nl202648p |*Nano Lett.* XXXX, XXX, 000–000

■ ASSOCIATED CONTENT

Supporting Information. Additional figures about the SEM of ZnO micro/nanowires, optical images of P3HT on the ZnO wire, schematic of the measuring system, $I-V$ characteristics of the fabricated devices of two contact types, $I-V$ characteristics of Ag−ZnO−Ag structures, AFM image of a single triangle ZnO wire, and the calculation of strain for the fabricated devices. This material is available free of charge via the Internet at http://pubs.acs.org.

■ AUTHOR INFORMATION

Corresponding Author
*E-mail: zlwang@gatech.edu.

■ ACKNOWLEDGMENT

This work was supported by BES DOE (DE-FG02-07ER46394). The authors thank Yusheng Zhou for assistance on AFM imaging.

■ REFERENCES

(1) Cui, Y.; Wei, Q.; Park, H.; Lieber, C. M. *Science* **2001**, *293*, 1289.
(2) Tian, B.; Cohen-Karni, T.; Qing, Q.; Duan, X.; Xie, P.; Lieber, C. M. *Science* **2010**, *329*, 831.
(3) Cui, Y.; Lieber, C. M. *Science* **2001**, *291*, 851.
(4) Wang, Z. L.; Song, J. H. *Science* **2006**, *312*, 242.
(5) Zhu, J.; Hsu, C.; Yu, Z.; Fan, S.; Cui, Y. *Nano Lett.* **2010**, *10*, 1979.
(6) Kempa, T. J.; Tian, B.; Kim, D. R.; Hu, J.; Zheng, X.; Lieber, C. M. *Nano Lett.* **2008**, *8*, 3456.
(7) Fan, Z. Y.; Lu, J. G. *Appl. Phys. Lett.* **2005**, *86*, 032111.
(8) Cheng, Y.; Xiong, P.; Fields, L.; Zheng, J. P.; Yang, R. S.; Wang, Z. L. *Appl. Phys. Lett.* **2006**, *89*, 093114.
(9) Zhu, H.; Shan, C.; Li, B.; Zhang, Z. Z.; Shen, D.; Choy, K. *J. Mater. Chem.* **2011**, *21*, 2848.
(10) Park, W. I.; Yi, G. C. *Adv. Mater.* **2004**, *16*, 87.
(11) Wei, Y.; Xu, C.; Xu, S.; Li, C.; W, W; Wang, Z. L. *Nano Lett.* **2010**, *10*, 2092.
(12) Yang, R.; Qin, Y.; Dai, L.; Wang, Z. L. *Nat. Nanotechnol.* **2009**, *4*, 34.
(13) He, J. H.; Hsin, C. L.; Liu, J.; Chen, L. J.; Wang, Z. L. *Adv. Mater.* **2007**, *19*, 781.
(14) Yang, Y.; Qi, J. J.; Liao, Q. L.; Li, H. F.; Wang, Y. S.; Tang, L. D.; Zhang, Y. *Nanotechnology* **2009**, *20*, 125201.
(15) Wang, X.; Zhou, J.; Song, J.; Liu, J.; Xu, N.; Wang, Z. L. *Nano Lett.* **2006**, *6*, 2768.
(16) Yang, Y.; Qi, J. J.; Guo, W.; Gu, Y. S.; Huang, Y. H.; Zhang, Y. *Phys. Chem. Chem. Phys.* **2010**, *12*, 12415.
(17) Zhou, J.; Gu, Y.; Fei, P.; Mai, W.; Gao, Y.; Yang, R.; Bao, G.; Wang, Z. L. *Nano Lett.* **2008**, *8*, 3035.
(18) Wu, W.; Wang, Z. L. *Nano Lett.* **2011**, *11*, 2779.
(19) Yang, Q.; Guo, X.; Wang, W.; Zhang, Y.; Xu, S.; Lien, D. H.; Wang, Z. L. *ACS Nano* **2010**, *4*, 6285.
(20) Hu, Y.; Zhang, Y.; Chang, Y.; Snyder, R. L.; Wang, Z. L. *ACS Nano* **2010**, *4*, 4220.
(21) Spoerke, E. D.; Lloyd, M. T.; McCready, E. M.; Olson, D. C.; Lee, Y. J.; Hsu, W. P. *Appl. Phys. Lett.* **2009**, *95*, 213506.
(22) Coakley, K. M.; McGehee, M. D. *Appl. Phys. Lett.* **2003**, *83*, 3380.
(23) Peiro, A. M.; Ravirajan, P.; Govender, K.; Boyle, D. S.; O'Brien, P.; Bradley, D. D. C.; Nelson, J.; Durrant, J. R. *J. Mater. Chem.* **2006**, *16*, 2088.
(24) Gao, J.; Luther, J. M.; Semonin, O. E.; Ellingson, R. J.; Nozik, A. J.; Beard, M. C. *Nano Lett.* **2011**, *11*, 1002.
(25) Oosterhout, S. D.; Wienk, M. M.; van Bavel, S. S.; Thiedmann, R.; Koster, L. J. A.; Gilot, J.; Loos, J.; Schmidt, V.; Janssen, R. A. J. *Nat. Mater.* **2009**, *8*, 818.
(26) Vaynzof, Y.; Kabra, D.; Zhao, L.; Ho, P. K. H.; Wee, A. T.-S.; Friend, R. H. *Appl. Phys. Lett.* **2010**, *97*, 033309.
(27) Olson, D. C.; Shaheen, S. E.; Collins, R. T.; Ginley, D. S. *J. Phys. Chem. C* **2007**, *111*, 16640.
(28) Lin, Y. Y.; Lee, Y. Y.; Chang, L.; Wu, J. J.; Chen, C. W. *Appl. Phys. Lett.* **2009**, *94*, 063308.
(29) Pan, Z. W.; Dai, Z. R.; Wang, Z. L. *Science* **2001**, *291*, 1947.
(30) Wu, W.; Wei, Y.; Wang, Z. L. *Adv. Mater.* **2010**, *22*, 4711.
(31) Xue, J.; Uchida, S.; Rand, B. P.; Forrest, S. R. *Appl. Phys. Lett.* **2004**, *84*, 3013.
(32) Ishwara, T.; Bradley, D. D. C.; Nelson, J.; Ravirajan, P.; Vanseveren, I.; Cleij, T.; Vanderzande, D.; Lutsen, L.; Tierney, S.; Heeney, M.; McCulloch, I. *Appl. Phys. Lett.* **2008**, *92*, 053308.
(33) Potscavage, W. J.; Yoo, J. S.; Kippelen, B. *Appl. Phys. Lett.* **2008**, *93*, 193308.
(34) Yang, Y.; Qi, J. J.; Zhang, Y.; Liao, Q. L.; Tang, L. D.; Qin, Z. *Appl. Phys. Lett.* **2008**, *92*, 183117.
(35) Han, X.; Kou, L.; Lang, X.; Xia, J.; Wang, N.; Qin, R.; Lu, J.; Xu, J.; Liao, Z.; Zhang, X.; Shan, X.; Song, X.; Gao, J.; Guo, W.; Yu, D. *Adv. Mater.* **2009**, *21*, 4937.
(36) Zhou, J.; Fei, P.; Gu, Y.; Mai, W.; Gao, Y.; Yang, R.; Bao, G.; Wang, Z. L. *Nano Lett.* **2008**, *8*, 3973.
(37) Zhang, Y.; Liu, Y.; Wang, Z. L. *Adv. Mater.* **2011**, *23*, 3004.
(38) Wang, Z. L. *Nano Today* **2010**, *5*, 540.
(39) Gao, Y. F.; Wang, Z. L. *Nano Lett.* **2009**, *9*, 1103.
(40) Gao, Z. Y.; Zhou, J.; Gu, Y. D.; Fei, P.; Hao, Y.; Bao, G.; Wang, Z. L. *J. Appl. Phys.* **2009**, *105*, 113707.
(41) Shao, Z.; Wen, L.; Wu, D.; Zhang, X.; Chang, S.; Qin, S. *J. Appl. Phys.* **2010**, *108*, 124312.